Dissemination Bottleneck in a Murine Model of Inhalational Anthrax

Roger D. Plaut, Vanessa K. Kelly, Gloria M. Lee, Scott Stibitz, and Tod J. Merkel

Division of Bacterial, Parasitic, and Allergenic Products, Center for Biologics Evaluation and Research, Food and Drug Administration, Bethesda, Maryland, USA

Inhalational anthrax is caused by the sporulating bacterium *Bacillus anthracis*. A current model for progression in mammalian hosts includes inhalation of bacterial spores, phagocytosis of spores in the nasal mucosa-associated lymphoid tissue (NALT) and lungs by macrophages and dendritic cells, trafficking of phagocytes to draining lymph nodes, germination of spores and multiplication of vegetative bacteria in the NALT and lymph nodes, and dissemination of bacteria via the bloodstream to multiple organs. In previous studies, the kinetics of infection varied greatly among mice, leading us to hypothesize the existence of a bottleneck past which very few spores (perhaps only one) progress to allow the infection to proceed. To test this hypothesis, we engineered three strains of *B. anthracis* Sterne, each marked with a different fluorescent protein, enabling visual differentiation of strains grown on plates. Mice were infected with a mixture of the three strains, the infection was allowed to proceed, and the strains colonizing the organs were identified. Although the inoculum consisted of approximately equal numbers of each of the three strains, the distal organs were consistently colonized by a majority of only one of the three strains, with the dominant strain varying among animals. Such dominance of one strain over the other two was also found at early time points in the cervical lymph nodes but not in the mediastinal lymph nodes. These results support the existence of a bottleneck in the infectious process.

The Gram-positive spore-forming bacterium *Bacillus anthracis* can cause three forms of anthrax illness in humans: cutaneous, gastrointestinal, and inhalational. Inhalational anthrax results from spores inhaled into the airway. This is the most severe form of the disease, often associated with rapid disease progression and death (4, 10, 35). The anthrax mail attacks of 2001 led to several cases of inhalational anthrax, including five deaths (18). Upon inhalation, anthrax spores are trapped in the nasal turbinates or reach the alveoli of the lung. It is generally believed that, following uptake by macrophages or dendritic cells, *B. anthracis* spores are carried by these phagocytic cells to lymphoid tissues, where they germinate and multiply within the macrophages or dendritic cells, resulting in lysis of the host cell and escape of the vegetative bacteria (8, 13–16). Vegetative cells multiply within the lymphoid tissues and gain entry into the bloodstream, resulting in the development of severe bacteremia (20, 30), followed by hematogenous spread of bacilli to multiple organs and lymph nodes (2, 3, 12). This leads to vascular injury with edema, hemorrhage, and thrombosis, ultimately resulting in the death of the host (7).

We previously described a mouse model of inhalational anthrax, in which A/J mice are infected with aerosolized spores of a capsule-negative (Sterne) strain of *B. anthracis* (21–23). This model recapitulates a number of important pathological features of anthrax infection of other mammalian hosts, including humans. Mice infected in these studies exhibited a time to death varying from 2 to 8 days. The use of a bioluminescent strain to image the progression of disease in living mice over time allowed us to observe asynchronous dissemination of the infection in individual animals (22).

The observation that disease progression beyond the lymphoid tissue occurs at significantly different times in different animals led us to hypothesize that a bottleneck exists in the pathway of infection and that only one or very few bacterial cells proceed past the bottleneck at one time. This bottleneck thus represents some rate-limiting step, after which these few bacterial cells can replicate rapidly, leading to disseminated infection. In an approach

used in previous studies that demonstrated a similar phenomenon in other infections (19, 24–26, 31, 32, 34, 36), we infected mice with a mixture of differentially marked but otherwise phenotypically identical strains. In the present case, we used a mixture of three strains, each marked with a fluorescent protein of a different color. We infected mice with a mixture of the three strains and followed the progression of the infection by bioluminescence imaging (BLI). Individual mice in which infection had disseminated were sacrificed, and the makeup of the bacterial populations in different tissues was determined. In each mouse in which the infection had disseminated, we found that CFU recovered from the kidneys were dominated by one strain over the other two, although the particular strain dominating varied among mice. When mice were sacrificed prior to dissemination of the infection, CFU recovered from the mediastinal lymph nodes (mLNs) were found to be a mixture of the three strains; however, CFU recovered from the cervical lymph nodes (cLNs) were dominated by one strain. These results strongly suggest the existence of a bottleneck prior to or in the cLNs. Additionally, these results are evidence of independent rather than cooperative action of *B. anthracis* in this animal model of inhalational anthrax.

MATERIALS AND METHODS

Bacterial strains and plasmids. Bacterial strains and plasmids are listed in Table 1. The plasmid pSS4530 (22) was used as the backbone for engineering luminescent and fluorescent strains of *B. anthracis* Sterne 7702. This

TABLE 1 Strains and plasmids used in this work

Plasmid or strain	Description/features	Reference or source
Plasmids		
pSS4530	Temperature-sensitive origin of replication; *luxBADCE* under the control of a constitutive promoter; ORF[a] BA1951	22
pRP1164	pSS4530 with codon-optimized TurboGFP	This work
pRP1191	pSS4530 with codon-optimized TurboYFP	This work
pRP1168	pSS4530 with codon-optimized TurboFP635	This work
B. anthracis strains		
BA663	Sterne 7702; pXO1$^+$ pXO2$^-$	5
BAP578	BA663 with integrated pRP1164	This work
BAP579	BA663 with integrated pRP1191	This work
BAP580	BA663 with integrated pRP1168	This work

[a] ORF, open reading frame.

plasmid carries the consensus trc-99 promoter, a modified *luxBADCE* operon from *Photorhabdus luminescens*, and the entire open reading frame of BA1951, to permit integration of the plasmid at that site. BA1951 encodes a nitroreductase-like protein under the control of the strong P_{ntr} (L-19) promoter (11). Integration of the plasmid by homologous recombination is expected to place the *luxBADCE* operon under the control of both the P_{ntr} promoter of BA1951 and the trc-99 promoter, without disrupting BA1951. Genes encoding fluorescent proteins codon optimized for expression in *B. anthracis* were synthesized (GenScript, Piscataway, NJ). The synthesized genes encoding TurboGFP (9), TurboYFP (Evrogen), and TurboFP635 (33) were digested with SalI and inserted at the XhoI site of pSS4530, generating plasmids pRP1164, pRP1191, and pRP1168, respectively. Plasmids were transferred to Sterne 7702 by conjugation, and integrants were selected by growth at 37°C in the presence of erythromycin as previously described (17). Following isolation of integrants, individual colonies were picked and passaged such that the three strains used in this study (BAP578, BAP579, and BAP580) exhibited luminescence of approximately the same intensity, as previously described (22).

Mouse infections. Spores were prepared as previously described (28). For mixed infections, equal numbers of spores of each strain were combined in 15 ml distilled H$_2$O with 0.01% Tween 80 to a final concentration of 5×10^9 spores/ml. Aerosol infection of A/J mice (Jackson Laboratory, Bar Harbor, ME), euthanization, tissue collection, and homogenization were performed as previously described (22). A portion of each homogenate was heat treated at 65°C for 30 min to kill vegetative bacilli. Homogenates were serially diluted and plated on brain heart infusion (BHI) agar plates containing 5 μg/ml erythromycin. Plates were incubated overnight at 37°C followed by 24 to 48 h of further incubation at room temperature (approximately 23°C) to allow for maturation of the fluorescent proteins before imaging. The lower limit of detection was 4 CFU for lymph node samples and 50 CFU for other organ samples. Plates with 30 to 300 colonies were used for enumeration and determination of the percentages of each of the three strains.

Imaging and image processing. To follow the progression of the infection, mice were imaged with an IVIS100 *in vivo* imaging system (Caliper Life Sciences, Hopkinton, MA) as previously described (22). Agar plates were imaged with an LAS-3000 imaging system (Fujifilm Medical Systems, Stamford, CT) with the following settings: for TurboGFP, blue light-emitting diode (LED), 510DF10 filter; for TurboYFP, green LED, 575DF20 filter; for TurboFP635, green LED, R670 filter. Images were false colored and merged using ImageJ (1). Images were adjusted for brightness

and contrast, and colonies were enumerated and identified by color using PhotoShop CS3 (Adobe Systems, San Jose, CA).

Statistical analysis. Data were analyzed using Prism, version 5.04 (GraphPad Software, La Jolla, CA). Maximum percentages of CFU of one strain recovered from organs were compared by the Kruskal-Wallis test followed by Dunn's multiple comparison test.

RESULTS

Development and initial characterization of test strains. We hypothesized that the bacteria colonizing distal organs in a disseminated infection of inhalational anthrax are the progeny of one or very few bacterial cells. In order to test this hypothesis, we developed three strains of *B. anthracis* Sterne that could be easily differentiated. Each strain was engineered to express a different fluorescent protein. Additionally, to facilitate tracking of the course of the infection with bioluminescence imaging (BLI), each of the three strains was engineered to carry the modified *lux* operon employed previously (22). The genes encoding the fluorescent proteins and the *lux* operon were features of plasmids that were integrated into the *B. anthracis* Sterne chromosome (as described in Materials and Methods), generating the three strains BAP578 (TurboGFP), BAP579 (TurboYFP), and BAP580 (TurboFP635).

The three strains exhibited no gross differences in kinetics of growth *in vitro* (Fig. 1A). To determine whether any of the strains
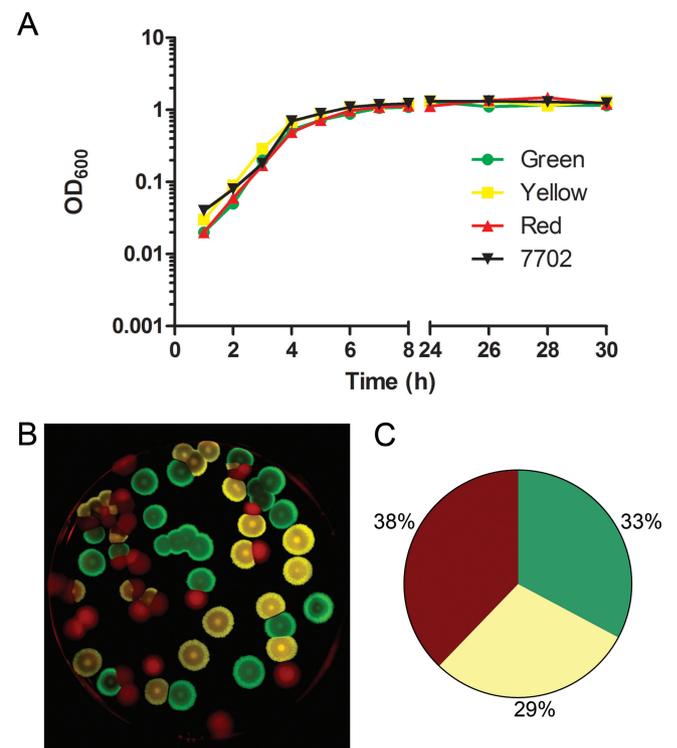

FIG 1 Analysis of *in vitro* growth. (A) *In vitro* growth curves. Strains were grown overnight in BHI with (fluorescent strains) or without (Sterne 7702) 5 μg/ml erythromycin and subcultured at a dilution of 1:100 in BHI without antibiotic. Green, BAP578 (TurboGFP); yellow, BAP579 (TurboYFP); red, BAP580 (TurboFP635); 7702, Sterne 7702. (B) Sample plate after *in vitro* outgrowth. Spores of the three strains were combined in a ratio of 1:1:1 and grown for 48 h in BHI containing 5 μg/ml erythromycin. Serial dilutions were plated on BHI agar containing 5 μg/ml erythromycin, and plates were imaged as described in Materials and Methods. The image was false colored using ImageJ software. (C) Percentages of each strain after *in vitro* outgrowth. Results are mean percentages from three replicates.
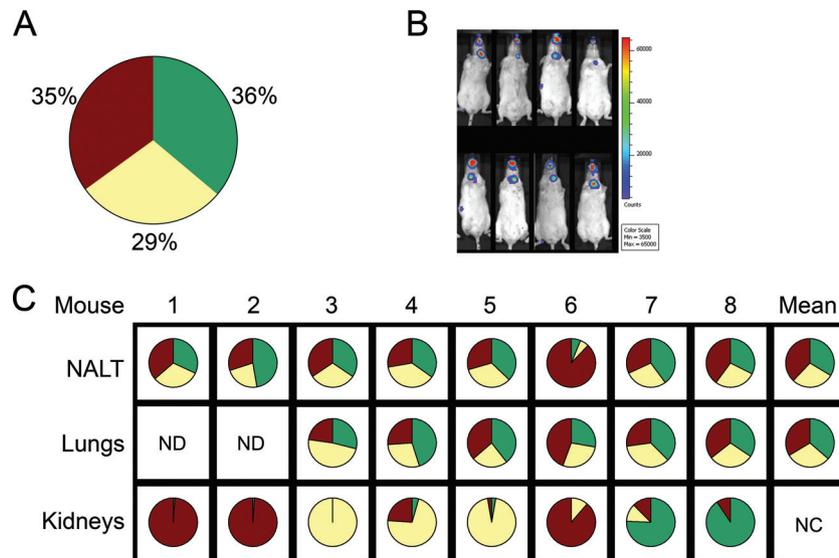
FIG 2 Aerosol infections with spore mixture. Mice were exposed to a 1:1:1 ratio of spores of the three strains. (A) Four hours after aerosol infection, four mice were sacrificed, NALT and lungs were harvested, and percent CFU of each strain recovered was calculated (green, BAP578; yellow, BAP579); red, BAP580; results shown are mean percentages from NALT and lungs of four mice. (B) The remaining mice were imaged and sacrificed when luminescence was apparent in the area of the cLNs. (C) For mice with more than 1,500 CFU detected in the kidneys, the percent CFU of each strain recovered from the organs was calculated; results shown are from one experiment. ND, no data; NC, not calculated.

possessed an *in vitro* growth advantage in a mixed culture, spores of the three strains were combined in a 1:1:1 ratio and allowed to germinate and grow in broth for 48 h, and dilutions were plated. Imaging using the appropriate conditions for the excitation and emission spectra of the three fluorescent proteins allowed the strains to be differentiated easily (Fig. 1B). The ratio of the strains recovered following overnight *in vitro* outgrowth did not vary substantially from the 1:1:1 starting mix (Fig. 1C).

Mixed infections. To address the hypothesized bottleneck during the dissemination of infection, mice were exposed to a mixture of spores of the three strains in a 1:1:1 ratio. A few animals were sacrificed 4 h later to characterize the delivered inoculum. Each of the three strains was found to represent approximately one-third of the CFU recovered from the nasal mucosa-associated lymphoid tissue (NALT) and lungs of these mice (Fig. 2A).

In the remaining animals, the progression of the infection was followed using BLI. When luminescence was observed in the area of the cLNs of a particular mouse (Fig. 2B), that animal was sacrificed, and CFU colonizing the organs were characterized (Fig. 2C). Mixtures recovered from the NALT and lungs usually remained near the 1:1:1 ratio of the inoculum, with some variability. In contrast, CFU recovered from the kidneys were nearly always dominated by one strain, although the particular strain that dominated varied among mice. Over the course of several experiments, in one-half of the mice (18/36), one strain represented 91 to 100% of the CFU recovered from the kidneys, while in the other mice, the predominant strain represented 51 to 90% of the CFU recovered from that site (Fig. 3A). The dominance of one strain over the other two in CFU recovered from the kidneys following dissemination was significantly different ($P < 0.001$) from the distribution of the three strains in the NALT and lungs of mice sacrificed 4 h after infection (Fig. 3B). These results strongly suggest the existence of a bottleneck at some prior point during the infection.

Spores initially deposited in the NALT are thought to be trans-

ported to the cLNs, whereas spores deposited in the lungs are expected to be transported to the mLNs. However, following dissemination of bacilli to distal sites, CFU recovered from the lymph nodes could represent a mixture of bacteria present early in infection and those reseeding the lymph nodes from the bloodstream. In order to evaluate the mixture of strains present in the lymph nodes prior to any possible reseeding with disseminated bacteria via the vasculature, the aerosol infection with the mixture of spores of the three strains was repeated, and 24 to 30 h later, all mice were sacrificed and CFU colonizing the cLNs, mLNs, kidneys, and livers were characterized. Of 30 mice infected in two separate experiments, six mice had no detectable CFU in the kidneys or liver but more than 120 CFU in either the cervical or the mediastinal lymph nodes (Fig. 4 and data not shown). In each of the animals for which over 120 CFU were detected in the cLNs but in which there was no detectable disseminated infection, there was over 50% dominance of one strain in the cLNs (Fig. 4, untreated homogenates). In contrast, in each of the mice in which over 120 CFU were detected in the mLNs, but in which there was no detectable disseminated infection, there was a relatively equal distribution of each of the three strains in the mLNs. These results suggest that there is likely a bottleneck prior to the cLNs but not prior to the mLNs.

As we observed previously (22), heat treatment of lymph node homogenates led to reductions in CFU, suggesting the presence of both spores and vegetative cells at those sites (Fig. 4). Because of the reduction in CFU of cLN homogenates following heat treatment, we were not able to reliably determine the ratios of spores of the three strains present in the cLNs. On the other hand, in four mice, data indicated that the three strains were equally represented in both untreated and heat-treated mLN homogenates, suggesting that there was no barrier to the transport of spores to the mLNs. Because we have not detected bacilli in the lungs at
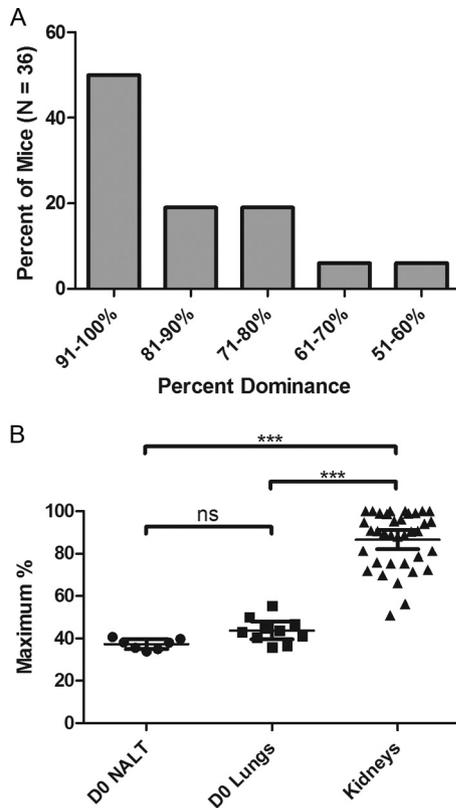
FIG 3 Extent of dominance in the kidneys. Mice were exposed to a 1:1:1 ratio of spores of the three strains. A few mice were sacrificed 4 h later, while the remaining mice were sacrificed when luminescence was apparent in the area of the cLNs. For organs from which more than 1,500 CFU were recovered, the percent CFU of each strain was calculated. (A) Mice were grouped together in the indicated ranges of percent dominance of one strain over the other two in the kidneys. (B) Comparison of the highest percent CFU of one color recovered from the NALT of mice sacrificed after 4 h (D0 NALT; $n = 7$), from the lungs of mice sacrificed after 4 h (D0 Lungs; $n = 10$), and from the kidneys of mice sacrificed when luminescence was apparent in the area of the cLNs ($n = 36$). Asterisks indicate P values of <0.001 between groups; ns, not statistically significant.

FIG 4 Percent CFU of each strain in lymph nodes prior to dissemination. Mice were exposed to a 1:1:1 ratio of spores of the three strains and sacrificed 24 to 30 h later. For the six mice with more than 120 CFU detected in the cLNs or mLNs but no detectable CFU in the kidneys or liver, the percent CFU of each strain was calculated. $n = 30$ mice infected in two experiments; HT, heat treated to kill vegetative bacilli; UT, untreated; <LOD, below lower limit of detection (4 CFU); <120 CFU, fewer than 120 CFU.

early time points, bacilli detected in the mLNs likely germinated there, or perhaps while en route to the mLNs from the lungs.

DISCUSSION

In our group's prior studies of inhalational anthrax, we found that the infection proceeded asynchronously among animals (21, 22). Despite being exposed to spores on the same day and receiving the same dose, mice exhibited a time to death that varied from 2 to 8 days after infection. Moreover, BLI data and CFU counts showed variation in the kinetics of progression of the infection among animals. These observations led us to hypothesize the existence of a barrier to the progression of infection and that passage of bacteria beyond such a barrier is a stochastic process. To investigate this possibility, we engineered three strains of *B. anthracis* Sterne that could be easily differentiated following a mixed infection. Results of mixed infections indicated a lack of a bottleneck in the lungs, NALT, and mLNs but the presence of a bottleneck in the pathway leading to infection of the cLNs, kidneys, and liver.

Dissemination of inhalational anthrax may occur via both the NALT and the lungs. We previously observed that, in this animal
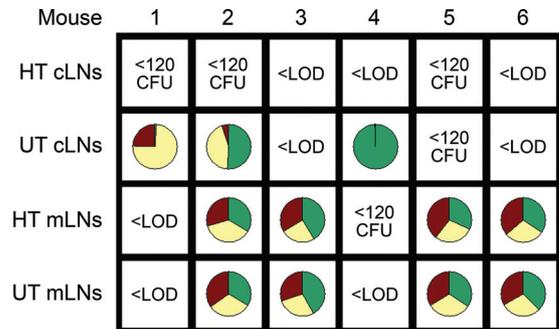
model of the illness, the first sites along these two pathways where vegetative bacilli can be detected are the NALT and mLNs (22). We note with interest that the bottleneck(s) occurs downstream of these two sites where germination first occurs. We found previously that dissemination beyond the NALT requires functional lethal toxin (LT) (22). Our interpretation of this result is that during an infection with a toxin-producing strain, the host response is engaged in the NALT but is unable to contain the infection in the face of LT activity. We speculate that, in the present study, the observed dominance of one strain in the cLNs results from replication of the first spore or bacillus to successfully break through this point in the host defenses.

The apparent bottleneck in this model of inhalational anthrax helps explain the observed asynchronous progression following inhalational infection. Studies using animal models of infection with pathogens such as *Streptococcus pneumoniae* (29) and *Yersinia pestis* (27) have reported similar results. In the latter case, the variability in the dissemination of *Y. pestis* among individual animals was attributed to variability in the timing of progression of the infection beyond the site of intraperitoneal injection. The stochastic nature of passage beyond a bottleneck (or multiple bottlenecks) could lead to the wide variability seen in the kinetics of progression among animals. Another implication of this finding is that methods commonly used to identify genes required *in vivo* (e.g., signature-tagged mutagenesis or transposon-site hybridization) are unlikely to be useful to study dissemination in this animal model. These methods require infection with a pool of mutant strains of bacteria, recovery of strains passing through the animal, and comparison of input and output pools. If only one or a few bacterial cells are responsible for the establishment of disseminated disease past the bottleneck, then identification of genes required for dissemination would not be possible using these methods (6).

The results described here have implications regarding the independent versus cooperative action of bacteria in this animal model (19, 24, 25). According to the independent action hypothesis, each bacterium acts alone and can cause infection; as the size of the inoculum is increased, the probability of infection occurring increases, because the probabilities of each bacterium causing infection are additive. Such a hypothesis contrasts with the coop-

erative action hypothesis, under which bacteria work together to cause infection; as the size of the inoculum is increased, the average probability per bacterium of causing infection increases, because of cooperation between individual bacteria. Recent reports supporting the independent action hypothesis include studies of a baculovirus-insect larva system, in which the frequency of dual-genotype infections was found to match predictions of the independent action model (36), and a mouse urinary tract infection caused by uropathogenic *Escherichia coli*, in which intracellular bacterial communities were determined to have arisen from a single bacterium (32). The presence of a bottleneck is consistent with independent action of individual bacteria in this model of inhalational anthrax, at least at some point during the progression to systemic disease, because apparently a single bacterium can be the founder of the disseminated infection. Therefore, prophylaxis, detection, and early intervention are extremely important for the prevention and treatment of this serious illness.

ACKNOWLEDGMENTS

REFERENCES

1. **Abramoff MD, Magalhaes PJ, Ram SJ.** 2004. Image processing with ImageJ. Biophotonics Int. **11**:36–42.
2. **Abramova FA, Grinberg LM, Yampolskaya OV, Walker DH.** 1993. Pathology of inhalational anthrax in 42 cases from the Sverdlovsk outbreak of 1979. Proc. Natl. Acad. Sci. U. S. A. **90**:2291–2294.
3. **Albrink WS.** 1961. Pathogenesis of inhalation anthrax. Bacteriol. Rev. **25**:268–273.
4. **Barnes JM.** 1947. The development of anthrax following administration of spores by inhalation. Br. J. Exp. Pathol. **28**:385–394.
5. **Cataldi A, Labruyère E, Mock M.** 1990. Construction and characterization of a protective antigen-deficient Bacillus anthracis strain. Mol. Microbiol. **4**:1111–1117.
6. **Chiang SL, Mekalanos JJ, Holden DW.** 1999. In vivo genetic analysis of bacterial virulence. Annu. Rev. Microbiol. **53**:129–154.
7. **Dalldorf FG, Kaufmann AF, Brachman PS.** 1971. Woolsorter's disease. Arch. Pathol. **92**:418–426.
8. **Dixon TC, Fadl AA, Koehler TM, Swanson JA, Hanna PC.** 2000. Early *Bacillus anthracis*-macrophage interactions: intracellular survival and escape. Cell. Microbiol. **2**:453–463.
9. **Evdokimov AG, et al.** 2006. Structural basis for the fast maturation of Arthropoda green fluorescent protein. EMBO Rep. **7**:1006–1012.
10. **Fritz DL, et al.** 1995. Pathology of experimental inhalation anthrax in the rhesus monkey. Lab. Invest. **73**:691–702.
11. **Gat O, et al.** 2003. Use of a promoter trap system in Bacillus anthracis and Bacillus subtilis for the development of recombinant protective antigen-based vaccines. Infect. Immun. **71**:801–813.
12. **Grinberg LM, Abramova FA, Yampolskaya OV, Walker DH, Smith JH.** 2001. Quantitative pathology of inhalational anthrax I: quantitative microscopic findings. Mod. Pathol. **14**:482–495.
13. **Guidi-Rontani C, Levy M, Ohayon H, Mock M.** 2001. Fate of germinated *Bacillus anthracis* spores in primary murine macrophages. Mol. Microbiol. **42**:931–938.
14. **Guidi-Rontani C, et al.** 1999. Identification and characterization of a germination operon on the virulence plasmid pXO1 of *Bacillus anthracis*. Mol. Microbiol. **33**:407–414.
15. **Guidi-Rontani C, Weber-Levy M, Labruyere E, Mock M.** 1999. Germination of *Bacillus anthracis* spores within alveolar macrophages. Mol. Microbiol. **31**:9–17.
16. **Ireland JA, Hanna PC.** 2002. Macrophage-enhanced germination of *Bacillus anthracis* endospores requires *gerS*. Infect. Immun. **70**:5870–5872.
17. **Janes BK, Stibitz S.** 2006. Routine markerless gene replacement in Bacillus anthracis. Infect. Immun. **74**:1949–1953.
18. **Jernigan DB, et al.** 2002. Investigation of bioterrorism-related anthrax, United States, 2001: epidemiologic findings. Emerg. Infect. Dis. **8**:1019–1028.
19. **Kunkel LO.** 1934. Tobacco and aucuba-mosaic infections by single units of virus. Phytopathology **24**:13.
20. **Lincoln RE, et al.** 1965. Role of lymphatics in the pathogenesis of anthrax. J. Infect. Dis. **115**:481–494.
21. **Loving CL, Kennett M, Lee GM, Grippe VK, Merkel TJ.** 2007. Murine aerosol challenge model of anthrax. Infect. Immun. **75**:2689–2698.
22. **Loving CL, et al.** 2009. Role of anthrax toxins in dissemination, disease progression, and induction of protective adaptive immunity in the mouse aerosol challenge model. Infect. Immun. **77**:255–265.
23. **Loving CL, et al.** 2009. Nod1/Nod2-mediated recognition plays a critical role in induction of adaptive immunity to anthrax after aerosol exposure. Infect. Immun. **77**:4529–4537.
24. **Meynell GG.** 1957. The applicability of the hypothesis of independent action to fatal infections in mice given Salmonella typhimurium by mouth. J. Gen. Microbiol. **16**:396–404.
25. **Meynell GG, Stocker BA.** 1957. Some hypotheses on the aetiology of fatal infections in partially resistant hosts and their application to mice challenged with Salmonella paratyphi-B or Salmonella typhimurium by intraperitoneal injection. J. Gen. Microbiol. **16**:38–58.
26. **Moxon ER, Murphy PA.** 1978. Haemophilus influenzae bacteremia and meningitis resulting from survival of a single organism. Proc. Natl. Acad. Sci. U. S. A. **75**:1534–1536.
27. **Nham T, Filali S, Danne C, Derbise A, Carniel E.** 2012. Imaging of bubonic plague dynamics by in vivo tracking of bioluminescent Yersinia pestis. PLoS One **7**:e34714. doi:10.1371/journal.pone.0034714.
28. **Pickering AK, Merkel TJ.** 2004. Macrophages release tumor necrosis factor alpha and interleukin-12 in response to intracellular bacillus anthracis spores. Infect. Immun. **72**:3069–3072.
29. **Rosch JW, Mann B, Thornton J, Sublett J, Tuomanen E.** 2008. Convergence of regulatory networks on the pilus locus of Streptococcus pneumoniae. Infect. Immun. **76**:3187–3196.
30. **Ross JM.** 1957. The pathogenesis of anthrax following the administration of spores by the respiratory route. J. Pathol. Bacteriol. **73**:485–494.
31. **Rubin LG.** 1987. Bacterial colonization and infection resulting from multiplication of a single organism. Rev. Infect. Dis. **9**:488–493.
32. **Schwartz DJ, Chen SL, Hultgren SJ, Seed PC.** 2011. Population dynamics and niche distribution of uropathogenic Escherichia coli during acute and chronic urinary tract infection. Infect. Immun. **79**:4250–4259.
33. **Shcherbo D, et al.** 2007. Bright far-red fluorescent protein for whole-body imaging. Nat. Methods **4**:741–746.
34. **Walters MS, et al.** 2012. Kinetics of uropathogenic Escherichia coli metapopulation movement during urinary tract infection. mBio **3**(1):e00303-11. doi:10.1128‡mBio. 00303-11.
35. **Zaucha GM, Pitt LM, Estep J, Ivins BE, Friedlander A.** 1998. The pathology of experimental anthrax in rabbits exposed by inhalation and subcutaneous inoculation. Arch. Pathol. Lab. Med. **122**:982–992.
36. **Zwart MP, et al.** 2009. An experimental test of the independent action hypothesis in virus-insect pathosystems. Proc. Biol. Sci. **276**:2233–2242.